

1  
2  
3  
4  
5  
6  
7 **Vitamin E promotes the inverse hexagonal phase**  
8 **via a novel mechanism: implications for**  
9  
10 **antioxidant role**  
11  
12  
13  
14  
15  
16  
17

18 Paul E. Harper,<sup>\*,†</sup> Andres T. Cavazos,<sup>‡</sup> Jacob J. Kinnun,<sup>‡,¶</sup> Horia I. Petrache,<sup>‡</sup>  
19  
20 and Stephen R. Wassall<sup>‡</sup>  
21  
22

23  
24 <sup>†</sup>*Department of Physics and Astronomy, Calvin University, Grand Rapids, MI, 49546-4403*

25  
26 <sup>‡</sup>*Department of Physics, IUPUI, Indianapolis, IN 46202-3273*

27  
28 <sup>¶</sup>*Current address: Department of Medicinal Chemistry and Molecular Pharmacology,*  
29  
30 *Purdue University, West Layayette, IN 47907*

31  
32  
33 E-mail: pharper@calvin.edu

34  
35 Phone: (616) 526-6408. Fax: (616) 526-6501  
36  
37  
38  
39  
40  
41  
42  
43  
44  
45  
46  
47  
48  
49  
50  
51  
52  
53  
54  
55

---

This is the author's manuscript of the article published in final edited form as:

Harper, P. E., Cavazos, A. T., Kinnun, J. J., Petrache, H. I., & Wassall, S. R. (2020). Vitamin E promotes the inverse hexagonal phase via a novel mechanism: Implications for antioxidant role. *Langmuir*. <https://doi.org/10.1021/acs.langmuir.0c00176>

## Abstract

Vitamin E ( $\alpha$ -tocopherol) and a range of other biological compounds have long been known to promote the  $H_{II}$  (inverted hexagonal) phase in lipids. Now, it has been well established that purely hydrophobic lipids such as dodecane promote the  $H_{II}$  phase by relieving *extensive* packing stress. They do so by residing deep within the hydrocarbon core. However, we argue from X-ray diffraction data obtained with 1-palmitoyl-2-oleoylphosphatidylcholine (POPE) and 1,2-dioleoylphosphatidylcholine (DOPE) that  $\alpha$ -tocopherol promotes the  $H_{II}$  phase by a different mechanism. The OH group on the chromanol moiety of  $\alpha$ -tocopherol anchors it near the aqueous interface. This restriction combined with the relatively short length of  $\alpha$ -tocopherol (compared to DOPE and POPE), means that  $\alpha$ -tocopherol promotes the  $H_{II}$  phase by relieving *compressive* packing stress. This observation offers new insight into the nature of packing stress and lipid biophysics. With the deeper understanding of packing stress offered by our results, we also explore the role molecular structure plays in the primary function of vitamin E, which is to prevent the oxidation of polyunsaturated membrane lipids.

## Introduction

The  $H_{II}$  or inverted hexagonal phase (See Fig. 1) in lipids has long been appreciated as a window offering insight into the both the biophysical properties of lipids and their interactions with proteins and other biomolecules.<sup>1</sup> The degree to which lipids curl, or their spontaneous curvature,<sup>2</sup> is revealed in the  $H_{II}$  phase and has been shown to exert a powerful effect on the conductance of the ion channel alamethicin.<sup>3</sup> Lung surfactant protein promotes curvature in the  $H_{II}$  phase and this is thought to be connected to its essential role for proper pulmonary function.<sup>4</sup> It is known that the wasp venom mastoparan promotes the  $H_{II}$  phase and that, interestingly, inhibitors of the venom do the reverse.<sup>5</sup> These are just a few examples of a whole host of membrane disruptive compounds, including anti-microbial peptides, that actively promote or inhibit the  $H_{II}$  phase.<sup>6,7</sup>

1  
2  
3  $\alpha$ -Tocopherol is the form of vitamin E retained by the human body. It is a lipid soluble  
4 antioxidant that is an essential micronutrient.<sup>8</sup> Symptoms of deficiency include nerve and  
5 muscle damage.<sup>9,10</sup> The primary role of  $\alpha$ -tocopherol is to protect polyunsaturated phos-  
6 pholipids from oxidation in membranes,<sup>11</sup> although modulation of membrane architecture is  
7 another mode of action that has recently been examined.<sup>12</sup> Its molecular structure consists  
8 of a chromanol group with a hydroxyl group on the benzene ring at one end and a phy-  
9 tanyl chain attached at the other end (See Fig. 2). In phospholipid bilayers, the hydroxyl  
10 group usually sits near the aqueous interface while the phytanyl chain extends towards the  
11 middle of the bilayer.<sup>13-16</sup> The effect of  $\alpha$ -tocopherol on the phospholipid is, somewhat akin  
12 to cholesterol, to disrupt chain packing in the gel state and to increase order in the liquid  
13 crystalline state.<sup>17,18</sup> Vitamin E is known to promote the H<sub>II</sub> phase.<sup>19-21</sup> Here we present  
14 data on phosphatidylethanolamine (PE) lipids that we propose reveals that  $\alpha$ -tocopherol  
15 induces the H<sub>II</sub> phase by a new mechanism.  
16  
17  
18  
19  
20  
21  
22  
23  
24  
25  
26  
27  
28

29 In terms of understanding the energetics of H<sub>II</sub> phase, there are two key components,  
30 namely the curvature energy and the packing energy. Following Gruner et al.<sup>2</sup> and more  
31 recent studies,<sup>22-26</sup> curvature energy represents an elastic free energy term that depends  
32 on bending rigidity and intrinsic curvature, while packing energy refers to hydrocarbon-  
33 packing free energy. The curvature energy is strongly influenced by the overall shape of  
34 the lipid and for lipids with high intrinsic curvature generally promotes curved phases such  
35 as H<sub>II</sub>. On the other hand, the anisotropy of lipid lengths in the H<sub>II</sub> phase gives rise to  
36 unfavorable packing energy (See Fig. 1). This foundational model was established by a  
37 classic series of experiments that showed a purely hydrophobic compound, such as dodecane,  
38 could relieve the packing stress by filling in the interstitial corners of the H<sub>II</sub> phase.<sup>2</sup> With  
39 the packing stress relieved, the curvature energy dominates and the lipid can express its  
40 spontaneous curvature.<sup>27</sup> This basic model has been used and extended with a great deal  
41 of success,<sup>28,29</sup> but open questions remain<sup>30</sup> and experimental measurements of curvature  
42 interactions remain an active area.<sup>24,31</sup>  
43  
44  
45  
46  
47  
48  
49  
50  
51  
52  
53  
54  
55  
56  
57  
58  
59  
60

1  
2  
3 We explore in this work the contrasting changes  $\alpha$ -tocopherol and dodecane make to the  
4  $H_{II}$  structure in POPE and DOPE and argue that these differences are due to the quite  
5 different interactions each compound has on lipids in general and the packing energy stress  
6 in particular.  
7  
8  
9  
10

## 11 12 13 **Materials and Methods**

### 14 15 16 **Sample Preparation**

17  
18  
19 POPE (16:0-18:1 PE or 1-palmitoyl-2-oleoyl-*sn*-glycero-3-phosphoethanolamine) and DOPE  
20 (18:1-18:1 PE or 1,2-dioleoyl-*sn*-glycero-3-phosphoethanolamine) were obtained from Avanti  
21 Polar Lipids (Alabaster, AL), while  $\alpha$ -tocopherol was prepared as previously described<sup>15</sup>  
22 and Sigma (St. Louis, MO) was the source for dodecane. Phospholipid (POPE or DOPE)  
23 was co-dissolved in chloroform with dodecane or  $\alpha$ -tocopherol in a 2:1 or 4:1 mol ratio,  
24 respectively. The organic solvent was removed under a stream of nitrogen gas followed by  
25 vacuum pumping overnight. The dried lipid was thoroughly mixed with water and was then  
26 transferred to an Eppendorf tube, with the final composition being 3 wt% lipid (approx.  
27 15 mg) in water. Samples containing  $\alpha$ -tocopherol were frozen and thawed three times to  
28 abet uniform dispersion before recording X-ray measurements. Samples containing dodecane  
29 were *not* frozen and thawed as we found this procedure actually resulted in the dodecane  
30 separating out, possibly due to dodecane's lower density. We note that freezing dodecane-  
31 lipid mixtures was not part of the mixing procedure in a previous X-ray study.<sup>32</sup> Equivalent  
32 mol, weight and volume compositions are listed in Table 1.  
33  
34  
35  
36  
37  
38  
39  
40  
41  
42  
43  
44  
45  
46  
47  
48  
49

### 50 51 **X-ray diffraction measurements**

52 X-ray diffraction data were taken using a fixed-anode Bruker Nanostar U system (Bruker  
53 AXS, Madison, WI), with a typical exposure being 14,400 seconds (4 hours) in duration.  
54 The integrated sum of three such exposures for POPE and  $\alpha$ -tocopherol at 40 °C is shown in  
55  
56  
57  
58  
59  
60

Fig. 3. The peaks were integrated using the software package FIT2D and were Lorentz and multiplicity corrected.<sup>33</sup> The peak amplitudes thereby extracted from the data are given in Table 2.

## Results

The H<sub>II</sub> phase is depicted in Fig. 1 and consists of a hexagonal unit cell in which a layer of lipids wraps around a cylindrical water core. The distance from the center of the cell to the edge is at a minimum along the short direction and a maximum along the long direction. The lattice spacing,  $a$ , is the distance between the centers of adjacent water cores or, equivalently, twice the distance from the center of the cell to the edge along the short direction. The radius of the water core is  $r_p$ ; it has been shown that it is located at the electron density maximum.<sup>32,34</sup> The thickness of the lipid layer varies from  $l_{min}$  to  $l_{max}$ , each of these being respectively measured along the short and long directions of the unit cell. The average lipid length,  $l_{ave}$ , is calculated using an area weighted average.<sup>33</sup> Consequently, the average lipid length assumes a value that yields roughly equal areas of compression and expansion (see Fig. 1).

X-rays scatter primarily off electrons and so diffraction data can be used to reconstruct the electron density of the lipid structures. Note that this method only gives relative electron density,  $\Delta\rho$ , where  $\rho_{electron} = \rho_{average} + \Delta\rho$ . The relative electron density can be reconstructed from the measured X-ray diffraction amplitudes and their phasings via

$$\Delta\rho = \sum_{\substack{h,k \text{ max} \\ (h,k) \neq (0,0)}} \alpha_{hk} F_{hk} \cos(\mathbf{b}_{hk} \cdot \mathbf{r}) \quad (1)$$

where  $h$  and  $k$  are the Miller indices and  $\mathbf{r}$  is position. The  $\alpha_{hk}$ ,  $F_{hk}$  and  $\mathbf{b}_{hk}$  terms are, respectively the phase, amplitude and reciprocal lattice vector for each pair of Miller indices. Electron density reconstructions were performed and the proper phasing was determined by selecting the most physically plausible combination; i.e., one that resulted in a uniform

1  
2  
3 electron density peak ring corresponding to the phospholipid heads, an electron density valley  
4 in the center for the water region and a deeper valley for the low electron density region of  
5 the hydrocarbon tails. For basic, detailed information on performing reconstructions, the  
6 reader is referred to Harper et al.<sup>33</sup> For recent, innovative work on reconstructions one  
7 can also consult Frewein et al.<sup>35</sup> The resulting phasings were in agreement with the rubric  
8 developed in Turner and Gruner,<sup>32</sup> which states that for  $r_p/a > 0.258$ , the correct phasing is  
9  $+, -, -, +, +, +, +$  and for  $0.237 < r_p/a < 0.258$ , the correct phasing is  $+, -, -, -, +, +, +$ .  
10 These phasing combinations are also in agreement with subsequent reconstructions of lipids  
11 in  $H_{II}$  phase.<sup>33,36,37</sup>

21 A 3-D plot of the relative electron density ( $\Delta\rho$ ) of POPE and  $\alpha$ -tocopherol at 40 °C is  
22 shown in Fig. 4 (left panel). The phospholipid headgroups form a fairly uniform peaked ring  
23 that steeply drops off in the hydrocarbon region. Slices of the electron density through the  
24 short and long directions (See Fig. 1) are also shown in Fig. 4 (right panel). Note that there  
25 is a good deal of rotational symmetry, which is typical for these systems. Nonetheless, there  
26 is a noticeable difference in the relative electron density along the short and long directions.  
27 The peak relative electron densities along each direction are designated  $\Delta\rho_{short}$  and  $\Delta\rho_{long}$ .  
28

35 Fig. 5 illustrates the contrasting effect that dodecane and  $\alpha$ -tocopherol have on the  
36 structural parameters derived from our data that characterize the  $H_{II}$  phase (see Table 3).  
37 It can be seen that dodecane slightly increases the lattice parameter,  $a$ , for DOPE, whereas  
38  $\alpha$ -tocopherol substantially reduces it (Fig. 5, left panel). A similar trend is apparent with  
39 POPE (Fig. 5, right panel). As alluded to earlier, the radius  $r_p$  of the water core is the  
40 average of the radii measured for the electron density maxima along the short and long  
41 directions. Both dodecane and  $\alpha$ -tocopherol reduce the value of  $r_p$  in DOPE (Fig. 6, left  
42 panel) and POPE (Fig. 6, right panel). The reduction is greater with  $\alpha$ -tocopherol than  
43 dodecane.  
44  
45  
46  
47  
48  
49  
50  
51

53 Geometry (see Fig. 1) readily suffices to determine the minimum length of the lipid  
54  
55  
56  
57  
58

monolayer,  $l_{min}$ , which is

$$l_{min} = a/2 - r_p \quad (2)$$

and the maximum length of the lipid monolayer,  $l_{max}$ , which is

$$l_{max} = \frac{a/2}{\cos \pi/6} - r_p \quad (3)$$

The average lipid length can be calculated by taking an area weighted average of the length of the lipid monolayer. Note that in this paper lipid includes both the membrane forming lipid (DOPE or POPE) and the additive (dodecane or  $\alpha$ -tocopherol). It can be shown<sup>33</sup> that the average lipid length is well approximated by

$$l_{ave} = (a/2 - r_p) \left[ 1.1084 + 0.0572 \left( \frac{r_p}{a/2 - r_p} - 1 \right) \right]. \quad (4)$$

We accordingly see that dodecane increases the average lipid length, as opposed to  $\alpha$ -tocopherol that leaves it generally unchanged (See Fig. 7).

The cross-section area per lipid  $A$  at the lipid-water interface (Fig. 1) can be found by

$$A = V_{total} \left( \frac{2\pi r_p}{\sqrt{3}a^2/2 - \pi r_p^2} \right), \quad (5)$$

where, as before,  $a$  is the lattice size,  $r_p$  is the water core radius and  $V_{total} = V_{lipid} + V_{additive}$ .<sup>33</sup> Note that this definition of the area per lipid follows a volumetric decomposition of the unit cell as introduced by Luzzati et al.<sup>1</sup> and shown in Fig. 1. Since the volume fraction for both additives is about 0.13 (See Table 1), we note that therefore  $V_{total} = V_{lipid} + 0.13 V_{total}$  and hence  $V_{total} = V_{lipid}/0.87$ . It is apparent that the area stays roughly the same with the addition of dodecane but, in contrast, increases with  $\alpha$ -tocopherol (See Fig. 8).

## Discussion

It has long been appreciated that the extension of lipids in the long direction in the  $H_{II}$  phase is energetically costly, with this cost being known as the packing energy.<sup>2</sup> What is less appreciated is that an essential consequence of this energetically costly extension in the long direction must be necessarily accompanied by similarly costly compression in the short direction (see Fig. 1). This is readily understood by the following argument. Overextension in the long direction can be relieved by shrinking the thickness of the lipid monolayer in the  $H_{II}$  unit cell. One would then expect that shrinking to continue until opposed by the energetic cost of compression along the short direction. A similar argument can be made by modeling the free energy of the lipid as a harmonic function of lipid length with the minimum sensibly located at the average lipid length. Then, both lipid lengths longer and shorter than the average would necessarily result in free energy costs.

### A. $\alpha$ -Tocopherol and dodecane stabilize the $H_{II}$ phase by different mechanisms

With this model in mind, we can consider how dodecane relieves packing strain and promotes the  $H_{II}$  phase. The wholly hydrophobic structure of dodecane ensures that it will be located in the tail region of the  $H_{II}$  phase as schematically depicted in Fig. 9 (middle panel). This location has been confirmed by neutron scattering experiments.<sup>38</sup> Consequently, it is not surprising that the interfacial area per lipid remains basically unchanged (See Table 4). Classic packing energy theory informs us that it alleviates stress in the long direction, thereby promoting the  $H_{II}$  phase.<sup>2</sup> Hence the dodecane should be primarily be located in this region (See Fig. 9). At this point, our deeper appreciation of the dual stresses of extension and compression can now lead us into a fuller understanding of the host lipid and dodecane structure. By effectively extending the lipid lengths (See Fig. 9, middle panel), the dodecane not only relieves the extension stress, but consequently also relaxes the compression stress,



1  
2  
3 allowing the lipid along the short direction to relax to its optimum value. This can be seen  
4 quantitatively in that the  $l_{min}$  for DOPE and dodecane matches the  $l_{ave}$  for DOPE only (See  
5 Table 4).  
6  
7

8  
9 Turning to  $\alpha$ -tocopherol, we see a rather different situation. Instead of increasing  $l_{max}$   
10 as dodecane does,  $l_{max}$  is reduced by  $\alpha$ -tocopherol (See Table 4). For this reason alone, it  
11 seems highly unlikely that  $\alpha$ -tocopherol works as a lipid length extender as dodecane does.  
12 Furthermore, though mostly non-polar,  $\alpha$ -tocopherol does have a polar OH group at its tip.  
13 This group would tend to locate in the vicinity of the aqueous interface,<sup>14-16,39</sup> suggesting  
14  $\alpha$ -tocopherol would not find an energetic minimum deep in the non-polar region as dodecane  
15 does. Support for this position is seen in the interfacial area per lipid, which goes up upon  
16 the addition of  $\alpha$ -tocopherol (See Fig. 8). Therefore, we propose that  $\alpha$ -tocopherol relieves  
17 stress and promotes the H<sub>II</sub> phase by replacing lipids along the short direction (See Fig. 9,  
18 right panel). As noted earlier, the extensive and compressive stresses are inter-locked - one  
19 drives the other - so that if one of the stresses is relieved, the other is also reduced. Hence  
20 by alleviating the compressive stress,  $\alpha$ -tocopherol allows a reduction in the extensive stress,  
21 resulting in a reduced  $l_{max}$ , which is what we observe (See Table 4).  
22  
23  
24  
25  
26  
27  
28  
29  
30  
31  
32  
33  
34

35 In addition to our central argument, there is a suggestive pattern in how the electron  
36 density head group maximum varies. We have calculated  $\Delta\rho_{long}/\Delta\rho_{short}$ , the ratio of the elec-  
37 tron density maximum along the long direction relative to the short direction. The electron  
38 density maximum is due to the electron dense phosphorous headgroups; with  $\alpha$ -tocopherol  
39 as the additive, these headgroups are displaced in the short direction, presumably resulting  
40 in a reduced electron density maximum. This would result in an increase in  $\Delta\rho_{long}/\Delta\rho_{short}$ ,  
41 which is what we see for our data in Table 4. However, the magnitude of the difference  
42 of this ratio between samples with and without  $\alpha$ -tocopherol is approximately equal to its  
43 uncertainty, making this only a suggestive observation in support of our model.  
44  
45  
46  
47  
48  
49  
50  
51  
52

53 We do not mean to imply, however, that his mechanism is exclusive to  $\alpha$ -tocopherol.  
54 Other lipophilic molecules that anchor a head group at the aqueous interface, such as choles-

1  
2  
3 terol also induce the formation of the  $H_{II}$  phase.<sup>22</sup> In fact, the contrasting effects of  $\alpha$ -  
4 tocopherol and dodecane might generalize to other similar chemical compounds.  
5  
6  
7

## 8 **Biological implications**

9  
10  
11 Vitamin E is a lipophilic antioxidant.<sup>11</sup> To protect lipids from oxidative attack is the primary  
12 function of this essential constituent in membranes and is also the basis for its use as a  
13 preservative in food and cosmetics. The chemistry involved, whereby the OH group on  
14 the chromanol group is sacrificed to terminate the chain of reactions by which the lipid  
15 peroxidation progresses, is well understood.<sup>40</sup> Whether there is a structural component that  
16 encourages proximity to polyunsaturated phospholipids, the lipid species most vulnerable  
17 to oxidation, remains an unanswered question.<sup>18</sup> The behavior of PE when vitamin E is  
18 introduced offers potential insight.  
19  
20  
21  
22  
23  
24  
25  
26

27  
28 Promotion of negative curvature is revealed by the reduction in temperature of the lamel-  
29 lar to  $H_{II}$  phase transition for POPE when  $\alpha$ -tocopherol is added. It has been suggested that  
30 membranes with intrinsic, negative curvature are less permeable to oxygen.<sup>41</sup> The impact  
31 of vitamin E on the local architecture of membranes around PE, thus, may contribute to  
32 prevention of oxidation. Interestingly, moreover, polyunsaturated fatty acids (PUFA) are  
33 often preferentially taken up into PE.<sup>42</sup> From the results presented here, we also can affirm  
34 that matching lipid lengths - avoiding hydrophobic mismatch - is a profound driving force  
35 behind lipid organization. It makes sense that in a lipid bilayer, as illustrated in Fig. 10,  
36  $\alpha$ -tocopherol will seek to be next to lipids of a similar length. As the length of the chain  
37 (12 carbons) in  $\alpha$ -tocopherol's tail is less than the chain in a typical membrane phospholipid  
38 (16-18 carbons), this means that  $\alpha$ -tocopherol will generally find its best match with mem-  
39 brane lipids that have effectively shorter chains (Fig. 9, middle panel). The projected length  
40 of PUFA chains is shorter because their multiple double bonds confer tremendous disorder<sup>43</sup>  
41 so, we suggest,  $\alpha$ -tocopherol will naturally gravitate towards polyunsaturated lipids (Fig.  
42 10).  
43  
44  
45  
46  
47  
48  
49  
50  
51  
52  
53  
54  
55  
56  
57  
58  
59  
60

## Conclusions

In summary, we present evidence from electron density reconstructions that  $\alpha$ -tocopherol promotes the H<sub>II</sub> phase in PE by a new means, by relieving compressive stress. This mechanism contrasts with the well studied means by which dodecane promotes the H<sub>II</sub> phase, which is by reducing extensive stress. Our findings give us new insight both into the nature of packing stress and the interactions of molecules within the lipid membrane, offering potential insight into the biological function of  $\alpha$ -tocopherol.

## Acknowledgements

Funding for Paul Harper from Calvin University and the Calvin University Alumni Association is gratefully acknowledged. Paul Harper is also thankful for IUPUI (Indiana University, Purdue University at Indianapolis) for hosting his sabbatical. We would also like to thank Matthew L. Link for making some additional electron density calculations and Samuel W. Canner for help with figure preparation.

Table 1: The molecular weight and density, respectively, are 744 *g* and 1.00 *g/cm*<sup>3</sup> (DOPE) and 718 *g* and 1.00 *g/cm*<sup>3</sup> (POPE), each at 50 °C.<sup>33,34,36</sup> The molecular weight and density, respectively, are 431 *g* and 0.9 ± 0.1 *g/cm*<sup>3</sup> ( $\alpha$ -tocopherol) and 170 *g* and 0.8 ± 0.1 *g/cm*<sup>3</sup> (dodecane).<sup>44</sup> Note that the equivalent compositions for DOPE and POPE are practically identical.

Lipid	Additive	Equivalent Compositions		
		Mole fraction	Weight fraction	Volume fraction
DOPE	$\alpha$ -tocopherol	0.20	0.13	0.13
POPE	$\alpha$ -tocopherol	0.20	0.13	0.14
DOPE	dodecane	0.33	0.10	0.13
POPE	dodecane	0.33	0.11	0.14

Table 2: Lorentz and multiplicity corrected amplitudes calculated from measured peak intensities in X-ray data. Amplitudes for our data have been normalized to the first order peak.<sup>a</sup> Data from Turner and Gruner<sup>32</sup> The phasing for these peaks is +, -, -, +, +, +, +, +, -, -. Uncertainties in the amplitudes are of order ±0.03 relative to the first peak.

	Temp.		Amplitudes								
	(°C)	(1,0)	(1,1)	(2,0)	(2,1)	(3,0)	(2,2)	(3,1)	(4,0)	(3,2)	(4,1)
POPE and $\alpha$ -tocopherol	40	1.00	1.00	0.83	0.18	0.21	0.14	0.15			
	50	1.00	0.95	0.81	0.16	0.22	0.20	0.13			
POPE and dodecane	40	1.00	0.84	0.71	0.00	0.31	0.23	0.17			
	50	1.00	0.81	0.69	0.04	0.17	0.20	0.14			
DOPE and $\alpha$ -tocopherol	40	1.00	0.68	0.66	0.00	0.00	0.09	0.06			
	50	1.00	0.64	0.62	0.00	0.00	0.11	0.08			
DOPE and dodecane <sup>a</sup>	40	0.97	0.64	0.58	0.02	0.09	0.18	0.15	0.05		
	50	0.97	0.61	0.56	0.02	0.07	0.17	0.15	0.05		
DOPE <sup>a</sup>	40	0.95	0.87	0.73	0.13	0.18	0.17	0.14	0.02	0.03	0.04
	50	0.97	0.84	0.71	0.09	0.16	0.17	0.14	0.03	0.02	0.02

Table 3: Dimensional parameters for the lipid and additive combinations measured in this study. See Fig. 1 for the geometric definitions of the parameters and the Results section for how the parameters were calculated. Note that the average lipid length,  $l_{ave}$ , includes both the lipid and additive (if present). Uncertainties for the linear quantities ( $a$ ,  $r_p$ ,  $l_{ave}$ ) are  $\pm 0.5$  Å, with the uncertainty for the volume being  $\pm 20$  Å<sup>3</sup> and for the area being  $\pm 2$  Å<sup>2</sup>.

Structural Parameters						
	Temperature (°C)	$a$ (Å)	$r_p$ (Å)	$V_{lipid}$ (Å <sup>3</sup> )	$l_{ave}$ (Å)	$A$ (Å <sup>2</sup> )
POPE and $\alpha$ -tocopherol	40	74.8	20.6	1185	18.8	50.2
	50	72.6	20.0	1190	18.3	52.0
POPE and dodecane	40	82.2	22.2	1185	21.1	44.1
	50	79.5	21.1	1190	20.8	44.5
DOPE and $\alpha$ -tocopherol	40	63.0	15.5	1230	17.7	51.4
	50	61.6	15.2	1238	17.3	53.0

Table 4: In depth comparative listing of DOPE H<sub>II</sub> dimensions for DOPE only and with either dodecane or  $\alpha$ -tocopherol at a single temperature (40 °C). Note that the lipid lengths include both the lipid and additive (if present). <sup>a</sup> Data from Turner and Gruner.<sup>32</sup> Uncertainties are as in Table 3, with the uncertainty in  $\Delta\rho_{long}/\Delta\rho_{short}$  being  $\pm 0.06$ .

Detailed DOPE Dimensions at 40 °C								
	$a$ (Å)	$r_p$ (Å)	$\Delta\rho_{long}/\Delta\rho_{short}$	$l_{ave}$ (Å)	$l_{min}$ (Å)	$l_{max}$ (Å)	$l_{max} - l_{min}$ (Å)	$A$ (Å <sup>2</sup> )
DOPE only <sup>a</sup>	71.0	19.6	1.09	17.8	15.9	21.4	5.5	47.9
DOPE and dodecane <sup>a</sup>	72.0	18.4	1.09	19.5	17.6	23.2	5.6	47.7
DOPE and $\alpha$ -tocopherol	63.0	15.5	1.15	17.7	16.0	20.8	4.9	51.4

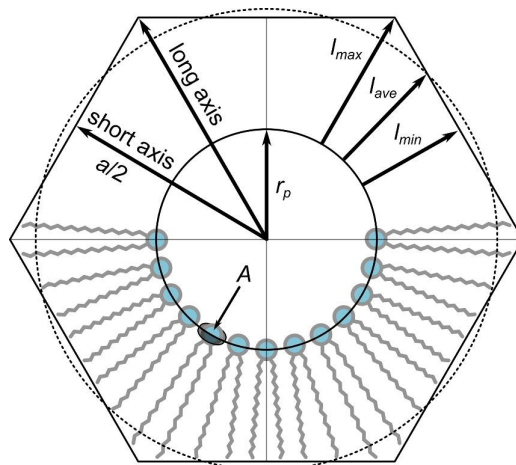
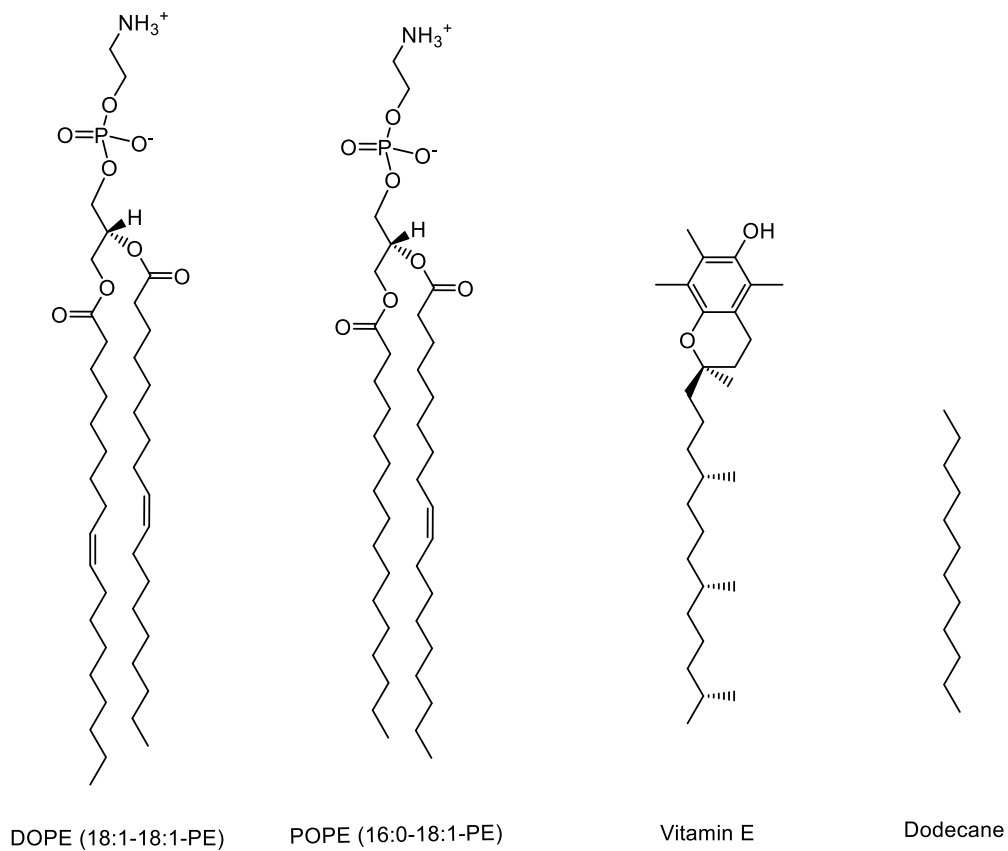


Figure 1: Diagram of a unit cell of the H<sub>II</sub> phase, which consists of a lipid monolayer wrapped around a cylindrical water core. Lipids are explicitly shown in the bottom half of the diagram, with the hydrophilic heads drawn as circles and the hydrophobic tails as zig-zag lines. Going from the center, one can get to the edge of the cell via the short path (which is one half of the lattice parameter  $a$ ) or via the long path. Lipid lengths are at a maximum,  $l_{max}$ , along the long path and a minimum,  $l_{min}$ , along the short path, with the average length,  $l_{ave}$ , lying in between. A circle with a radius equal to  $r_p + l_{ave}$  is drawn with a dashed line. The radius of the water core is  $r_p$  and the average cross sectional area per lipid at the Luzzati interface is  $A$ .



45 Figure 2: Chemical structures of DOPE, POPE,  $\alpha$ -tocopherol and dodecane.  
46  
47  
48  
49  
50  
51  
52  
53  
54  
55  
56  
57  
58  
59  
60

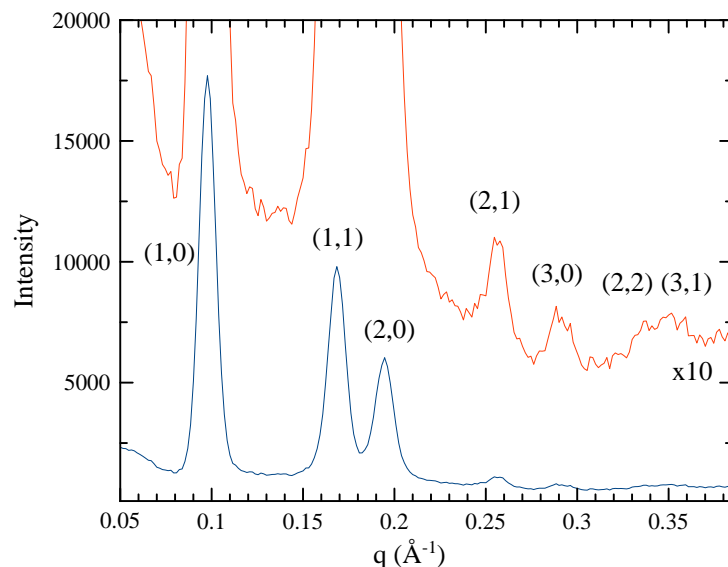


Figure 3: Integrated X-ray scattering intensity of POPE and  $\alpha$ -tocopherol at 40 °C. The scattering pattern is typical for the  $H_{II}$  phase and each peak is labeled by its Miller indices. The intensity x10 is also plotted to better reveal the weaker, higher order peaks.

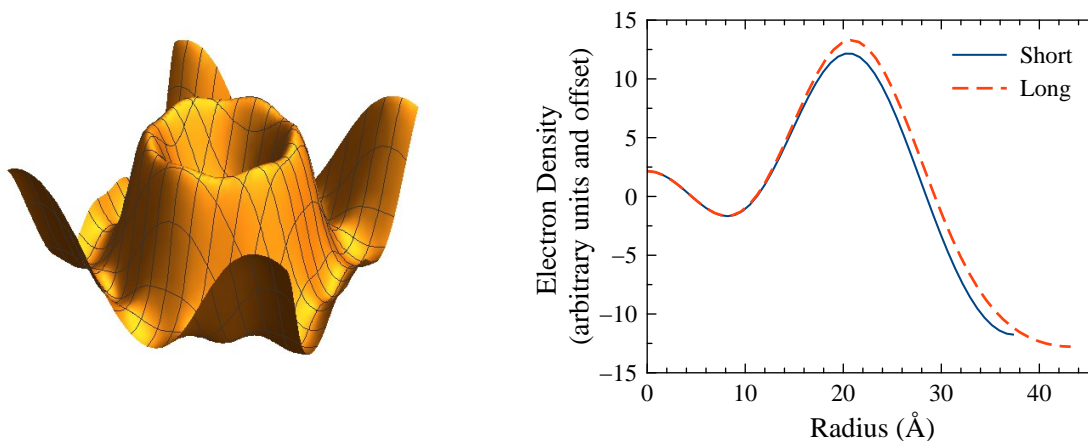


Figure 4: Relative electron density of POPE and  $\alpha$ -tocopherol at 40 °C. Left: 3-D plot of the electron density (vertical axis) of the  $H_{II}$  phase. The high electron density phospholipid headgroups generate a ring peak with a shallow inner central valley for the aqueous region and a deeper outer valley for the hydrocarbon region. Right: Slices of the electron density along the short and long directions (See Fig. 1). Note that the relative electron density maximum along the long direction ( $\Delta\rho_{long}$ ) is slightly higher than the electron density maximum along the short direction ( $\Delta\rho_{short}$ ).



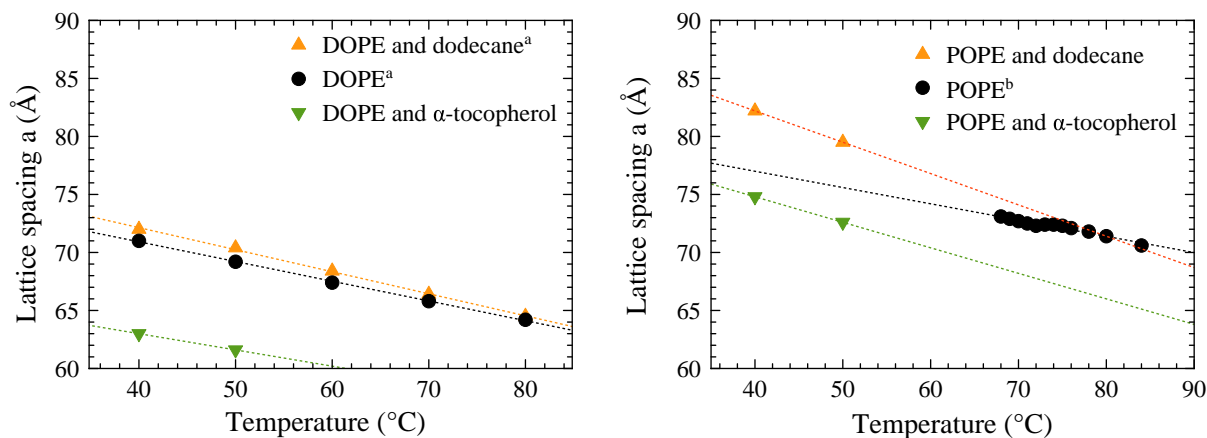


Figure 5: Lattice spacings (center of water core to center of water core distance) for DOPE (left) and POPE (right) for the lipid only, lipid with  $\alpha$ -tocopherol and lipid with dodecane. Linear fits of the data are displayed as dotted lines to guide the eye. For both DOPE and POPE,  $\alpha$ -tocopherol reduces the lattice spacing while dodecane increases it. <sup>a</sup> Data from Turner and Gruner.<sup>32</sup> <sup>b</sup> Data from Rappolt et al.<sup>36</sup>

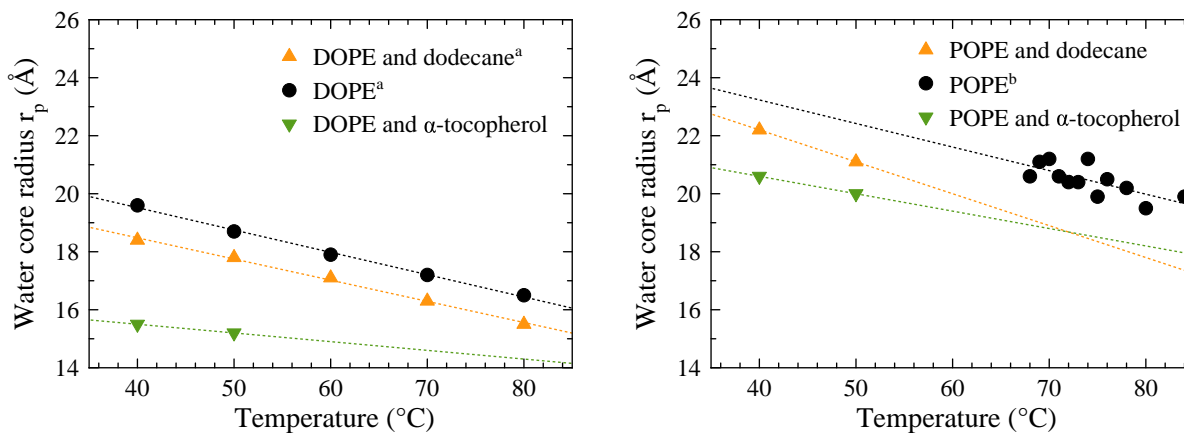


Figure 6: Water core radii for DOPE (left) and POPE (right) for the lipid only, lipid with  $\alpha$ -tocopherol and lipid with dodecane. Linear fits of the data are displayed as dotted lines to guide the eye. For both DOPE and POPE, the water core radius is reduced by  $\alpha$ -tocopherol and, to a lesser amount, dodecane. <sup>a</sup> Data from Turner and Gruner.<sup>32</sup> <sup>b</sup> Data from Rappolt et al.<sup>36</sup>

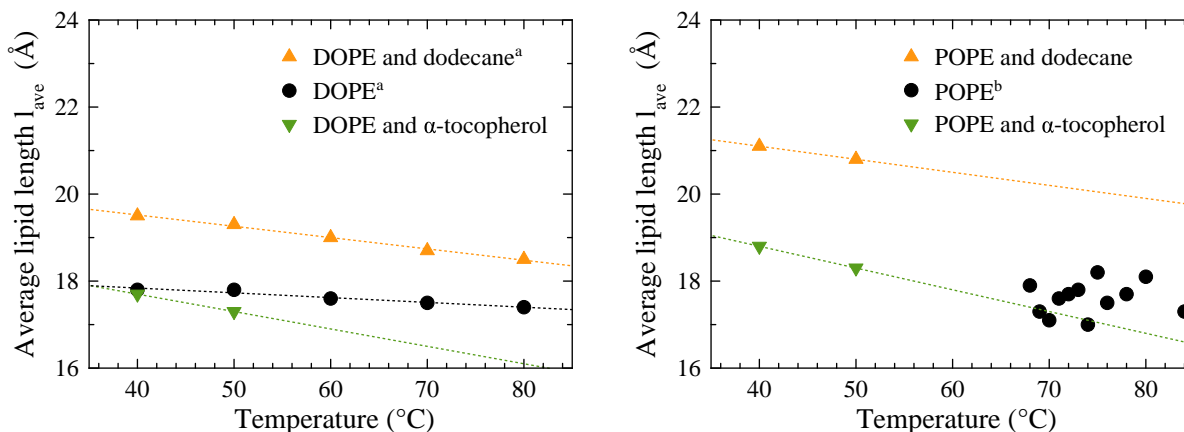


Figure 7: Average lipid lengths for DOPE (left) and POPE (right) for the lipid only, lipid with  $\alpha$ -tocopherol and lipid with dodecane. Linear fits of the data are displayed as dotted lines to guide the eye. For both DOPE and POPE,  $\alpha$ -tocopherol does not substantially change the average length but dodecane increases it. <sup>a</sup> Data from Turner and Gruner.<sup>32</sup> <sup>b</sup> Data from Rappolt et al.<sup>36</sup>

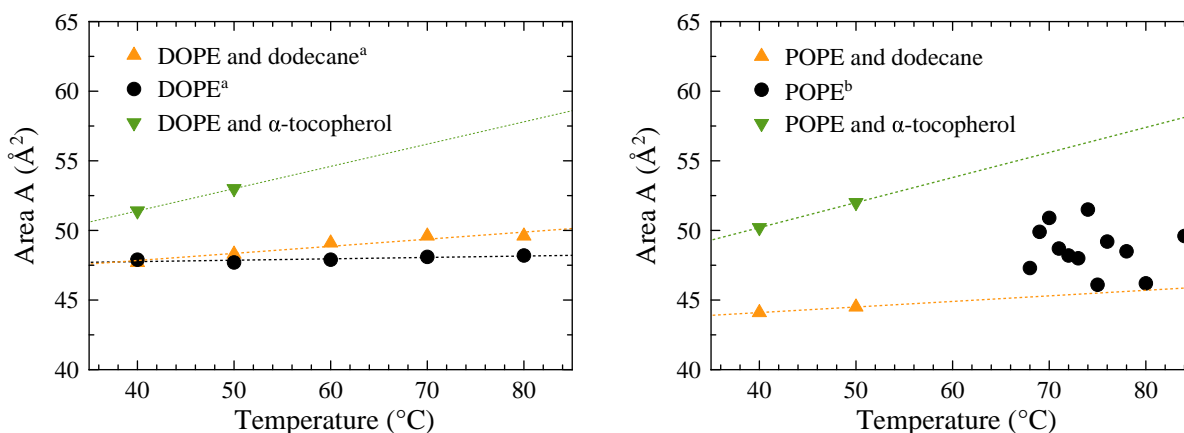


Figure 8: Average areas for DOPE (left) and POPE (right) for the lipid only, lipid with  $\alpha$ -tocopherol and lipid with dodecane. Linear fits of the data are displayed as dotted lines to guide the eye. In general,  $\alpha$ -tocopherol increases the area while dodecane does not seem to greatly change it. <sup>a</sup> Data from Turner and Gruner.<sup>32</sup> <sup>b</sup> Data from Rappolt et al.<sup>36</sup>

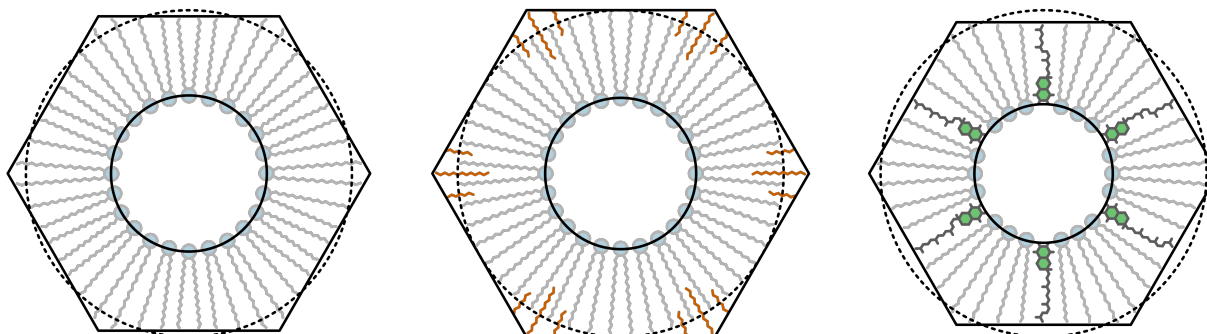


Figure 9: Models for PE only, PE and dodecane and PE and  $\alpha$ -tocopherol in the  $H_{II}$  phase. Dodecane fits in deep in the hydrocarbon tail region, predominately along the long direction. By contrast,  $\alpha$ -tocopherol fills in along the short direction and is relatively close to the lipid water interface. For all of the diagrams, the dashed circle indicates the average lipid length found in the PE only case. As discussed in the text, dodecane enlarges the unit cell so that the average lipid length in the PE only case matches the minimum lipid length in the PE and dodecane case. Likewise,  $\alpha$ -tocopherol reduces the unit cell size and the average lipid length for the PE only case is closer to the maximum lipid length in the PE and  $\alpha$ -tocopherol case.

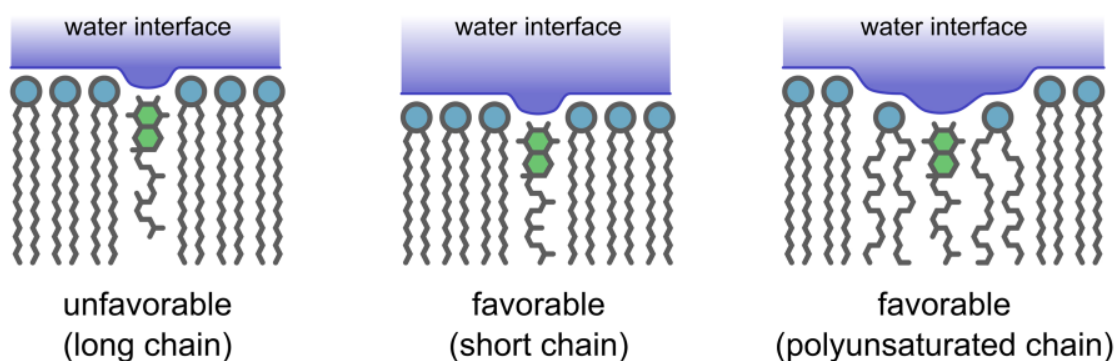


Figure 10: Model for the location of  $\alpha$ -tocopherol in a membrane. A single monolayer is shown. The location is unfavorable when there is a mismatch between chain length (left panel) and favorable when chain lengths match (middle panel). In a mixed membrane,  $\alpha$ -tocopherol locates next to polyunsaturated phospholipids in order to match chain length (right panel).

## References

- (1) Luzzati, V.; Reiss-Husson, F.; Rivas, E.; Gulik-Krzywicki, T. Structure and polymorphism in lipid-water systems, and their possible biological implications. *Ann. N. Y. Acad. Sci.* **1966**, *137*, 409–413.
- (2) Gruner, S. M. Intrinsic curvature hypothesis for biomembrane lipid composition: a role for nonbilayer lipids. *Proc. Natl. Acad. Sci. USA.* **1985**, *82*, 3665–3669.
- (3) Keller, S. L.; Bezrukov, S. M.; Gruner, S. M.; Tate, M. W.; Vodyanoy, I.; Parsegian, V. A. Probability of alamethicin conductance states varies with nonlamellar tendency of bilayer phospholipids. *Biophys. J.* **1993**, *65*, 23–27.
- (4) Chavarha, M.; Loney, R.; Rananavare, S.; Hall, S. Hydrophobic Surfactant Proteins Strongly Induce Negative Curvature. *Biophys. J.* **2015**, *109*, 95–105.
- (5) Tytler, E. M.; Segrest, J. P.; Epanand, R. M.; Nie, S. Q.; Epanand, R. F.; Mishra, V. K.; Venkatachalapathi, Y. V.; Anantharamaiah, G. M. Reciprocal effects of apolipoprotein and lytic peptide analogs on membranes. Cross-sectional molecular shapes of amphipathic alpha helices control membrane stability. *J. Biol. Chem.* **1993**, *268*, 22112–22118.
- (6) Epanand, R. M. Lipid polymorphism and protein–lipid interactions. *Biochim. Biophys. Acta* **1998**, *1376*, 353–368.
- (7) Hickel, A.; Danner-Pongratz, S.; Amenitsch, H.; Degovics, G.; Rappolt, M.; Lohner, K.; Pabst, G. Influence of antimicrobial peptides on the formation of nonlamellar lipid mesophases. *Biochim. Biophys. Acta* **2008**, *1778*, 2325–2333.
- (8) Niki, E.; Traber, M. G. A history of Vitamin E. *Annals of Nutrition and Metabolism* **2012**, *61*, 207–212.

- 1  
2  
3 (9) Traber, M. G. Vitamin E inadequacy in humans: causes and consequences. *Advances*  
4 *in nutrition* **2014**, *5*, 503–514.  
5  
6  
7  
8 (10) Ulatowski, L. M.; Manor, D. Vitamin E and neurodegeneration. *Neurobiology of disease*  
9 **2015**, *84*, 78–83.  
10  
11  
12 (11) Traber, M. G.; Atkinson, J. Vitamin E, antioxidant and nothing more. *Free Radical*  
13 *Biol. Med.* **2007**, *43*, 4–15.  
14  
15  
16 (12) DiPasquale, M.; Nguyen, M. H. L.; Rickeard, B. W.; Cesca, N.; Tannous, C.;  
17 Castillo, S. R.; Katsaras, J.; Kelley, E. G.; Heberle, F. A.; Marquardt, D. The an-  
18 tioxidant vitamin E as a membrane raft modulator: Tocopherols do not abolish lipid  
19 domains. *Biochimica et Biophysica Acta (BBA) - Biomembranes* **2020**, 183189.  
20  
21  
22 (13) Atkinson, J.; Epand, R. F.; Epand, R. M. Tocopherols and tocotrienols in membranes:  
23 A critical review. *Free Radical Biol. Med.* **2008**, *44*, 739–764.  
24  
25  
26 (14) Marquardt, D.; Kucerka, N.; Katsaras, J.; Harroun, T. A.  $\alpha$ -Tocopherol's location in  
27 membranes is not affected by their composition. *Langmuir* **2015**, *31*, 4464–4472.  
28  
29  
30 (15) Leng, X.; Kinnun, J. J.; Marquardt, D.; Ghefli, M.; Kučerka, N.; Katsaras, J.; Atkin-  
31 son, J.; Harroun, T. A.; Feller, S. E.; Wassall, S. R.  $\alpha$ -Tocopherol is well designed  
32 to protect polyunsaturated phospholipids: MD simulations. *Biophys. J.* **2015**, *109*,  
33 1608–1618.  
34  
35  
36 (16) Ausili, A.; de Godos, A. M.; Torrecillas, A.; Aranda, F. J.; Corbalan-Garcia, S.; Gomez-  
37 Fernandez, J. C. The vertical location of  $\alpha$ -tocopherol in phosphatidylcholine mem-  
38 branes is not altered as a function of the degree of unsaturation of the fatty acyl  
39 chains. *Phys. Chem. Chem. Phys.* **2017**, *19*, 6731–6742.  
40  
41  
42 (17) Suzuki, Y. J.; Tsuchiya, M.; Wassall, S. R.; Choo, Y. M.; Govil, G.; Kagan, V. E.;  
43 Packer, L. Structural and dynamic membrane properties of alpha-tocopherol and. alpha-  
44  
45  
46  
47  
48  
49  
50  
51  
52  
53  
54  
55  
56  
57  
58  
59  
60

- 1  
2  
3 tocotrienol: Implication to the molecular mechanism of their antioxidant potency. *Bio-*  
4 *chemistry* **1993**, *32*, 10692–10699.  
5  
6  
7
- 8 (18) Atkinson, J.; Harroun, T.; Wassall, S. R.; Stillwell, W.; Katsaras, J. The location and  
9 behavior of  $\alpha$ -tocopherol in membranes. *Mol. Nutr. Food Res.* **2010**, *54*, 641–651.  
10  
11  
12
- 13 (19) Nakajima, K.; Utsumi, H.; Kazama, M.; Hamada, A.  $\alpha$ -Tocopherol-Induced Hexagonal  
14  $H_{II}$  Phase Formation in Egg Yolk Phosphatidylcholine Membranes. *Chem. Pharm.*  
15 *Bull.* **1990**, *38*, 1–4.  
16  
17  
18
- 19 (20) Bradford, A.; Atkinson, J.; Fuller, N.; Rand, R. The effect of vitamin E on the structure  
20 of membrane lipid assemblies. *J. Lipid Res.* **2003**, *44*, 1940–1945.  
21  
22  
23
- 24 (21) Wang, X.; Quinn, P. J. The structure and phase behaviour of  $\alpha$ -tocopherol-rich domains  
25 in 1-palmitoyl-2-oleoyl-phosphatidylethanolamine. *Biochimie* **2006**, *88*, 1883–1888.  
26  
27  
28
- 29 (22) Kollmitzer, B.; Heftberger, P.; Rappolt, M.; Pabst, G. Monolayer spontaneous curva-  
30 ture of raft-forming membrane lipids. *Soft Matter* **2013**, *9*, 10877–10884, Kollmitzer,  
31 Benjamin Heftberger, Peter Rappolt, Michael Pabst, Georg.  
32  
33  
34  
35
- 36 (23) Perutkova, S.; Daniel, M.; Rappolt, M.; Pabst, G.; Dolinar, G.; Kralj-Iglic, V.; Iglic, A.  
37 Elastic deformations in hexagonal phases studied by small-angle X-ray diffraction and  
38 simulations. *Phys. Chem. Chem. Phys.* **2011**, *13*, 3100–3107.  
39  
40  
41  
42
- 43 (24) Tang, T. Y. D.; Brooks, N. J.; Ces, O.; Seddon, J. M.; Templer, R. H. Structural studies  
44 of the lamellar to bicontinuous gyroid cubic (Q(II)(G)) phase transitions under limited  
45 hydration conditions. *Soft Matter* **2015**, *11*, 1991–1997.  
46  
47  
48  
49
- 50 (25) Campelo, F.; Arnarez, C.; Marrink, S.; Kozlov, M. Helfrich model of membrane bend-  
51 ing: From Gibbs theory of liquid interfaces to membranes as thick anisotropic elastic  
52 layers. *Adv. Colloid Interface Sci.* **2014**, *208*, 25–33.  
53  
54  
55  
56  
57  
58  
59  
60

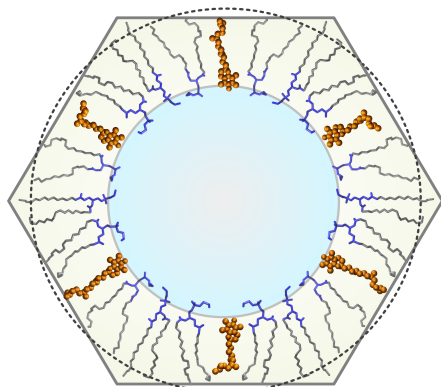
- 1  
2  
3 (26) Siegel, D. Fourth-Order Curvature Energy Model for the Stability of Bicontinuous In-  
4 verted Cubic Phases in Amphiphile-Water Systems. *Langmuir* **2010**, *26*, 8673–8683.  
5  
6  
7  
8 (27) Tate, M. W.; Eikenberry, E. F.; Turner, D. C.; Shyamsunder, E.; Gruner, S. M. Non-  
9 bilayer phases of membrane lipids. *Chem. Phys. Lipids* **1991**, *57*, 147–164.  
10  
11  
12 (28) Kozlov, M. M.; Leikin, S.; Rand, R. P. Bending, hydration and interstitial energies  
13 quantitatively account for the hexagonal-lamellar-hexagonal reentrant phase transition  
14 in dioleoylphosphatidylethanolamine. *Biophys. J.* **1994**, *67*, 1603–1611.  
15  
16  
17 (29) Duesing, P. M.; Templer, R. H.; Seddon, J. M. Quantifying packing frustration energy  
18 in inverse lyotropic mesophases. *Langmuir* **1997**, *13*, 351–359.  
19  
20  
21 (30) Shearman, G.; Ces, O.; Templer, R. Towards an understanding of phase transitions be-  
22 tween inverse bicontinuous cubic lyotropic liquid crystalline phases. *Soft Matter* **2010**,  
23 *6*, 256–262.  
24  
25  
26 (31) Reese, C. W.; Strango, Z. I.; Dell, Z. R.; Tristram-Nagle, S.; Harper, P. E. Structural  
27 insights into the cubic-hexagonal phase transition kinetics of monoolein modulated by  
28 sucrose solutions. *Phys. Chem. Chem. Phys.* **2015**, *17*, 9194–9204.  
29  
30  
31 (32) Turner, D. C.; Gruner, S. M. X-ray diffraction reconstruction of the inverted hexagonal  
32 (HII) phase in lipid-water systems. *Biochemistry* **1992**, *31*, 1340–1355.  
33  
34  
35 (33) Harper, P. E.; Mannock, D. A.; Lewis, R. N. A. H.; McElhaney, R. N.; Gruner, S. M.  
36 X-ray diffraction structures of some phosphatidylethanolamine lamellar and inverted  
37 hexagonal phases. *Biophys. J.* **2001**, *81*, 2693–2706.  
38  
39  
40 (34) Tate, M. W.; Gruner, S. M. Temperature dependence of the structural dimensions of the  
41 inverted hexagonal (HII) phase of phosphatidylethanolamine-containing membranes.  
42  
43  
44  
45  
46  
47  
48  
49  
50  
51  
52  
53  
54  
55  
56  
57  
58  
59  
60

- 1  
2  
3 (35) Frewein, M. P. K.; Rumetshofer, M.; Pabst, G. Global small-angle scattering data  
4 analysis of inverted hexagonal phases. *J. Appl. Crystallogr.* **2019**, *52*, 403–414.  
5  
6  
7  
8 (36) Rappolt, M.; Hickel, A.; Bringezu, F.; Lohner, K. Mechanism of the Lamellar/Inverse  
9 Hexagonal Phase Transition Examined by High Resolution X-Ray Diffraction. *Biophys.*  
10 *J.* **2003**, *84*, 3111–3122.  
11  
12  
13  
14 (37) Rappolt, M.; Hodzic, A.; Sartori, B.; Ollivon, M.; Laggner, P. Conformational and  
15 hydration properties during the  $L_{\beta}$ - to  $L_{\alpha}$ - and  $L_{\alpha}$ - to  $H_{II}$ -phase transition in phos-  
16 phatidylethanolamine. *Chem. Phys. Lipids* **2008**, *154*, 46–55.  
17  
18  
19  
20 (38) Turner, D. C.; Gruner, S. M.; Huang, J. S. Distribution of decane within the unit-cell  
21 of the inverted hexagonal (HII) phase of lipid water decane systems determined by  
22 neutron-diffraction. *Biochemistry* **1992**, *31*, 1356–1363.  
23  
24  
25  
26 (39) Qin, S.-S.; Yu, Z.-W.; Yu, Y.-X. Structural and Kinetic Properties of  $\alpha$ -Tocopherol  
27 in Phospholipid Bilayers, a Molecular Dynamics Simulation Study. *The Journal of*  
28 *Physical Chemistry B* **2009**, *113*, 16537–16546.  
29  
30  
31  
32 (40) Burton, G.; Ingold, K. U. Vitamin E: application of the principles of physical organic  
33 chemistry to the exploration of its structure and function. *Acc. Chem. Res.* **1986**, *19*,  
34 194–201.  
35  
36  
37 (41) Li, Q.-T.; Yeo, M. H.; Tan, B. K. Lipid peroxidation in small and large phospholipid  
38 unilamellar vesicles induced by water-soluble free radical sources. *Biochem. Biophys.*  
39 *Res. Commun.* **2000**, *273*, 72–76.  
40  
41  
42 (42) Wassall, S. R.; Stillwell, W. Polyunsaturated fatty acid–cholesterol interactions: domain  
43 formation in membranes. *Biochim. Biophys. Acta* **2009**, *1788*, 24–32.  
44  
45  
46 (43) Stillwell, W.; Wassall, S. R. Docosahexaenoic acid: membrane properties of a unique  
47 fatty acid. *Chem. Phys. Lipids* **2003**, *126*, 1–27.  
48  
49  
50  
51  
52  
53  
54  
55  
56  
57  
58  
59  
60



1  
2  
3 (44) ChemScr, CAS Number Index. <http://www.chemsrc.com/en/casindex/>, 2018.  
4  
5  
6  
7  
8  
9  
10  
11  
12  
13  
14  
15  
16  
17  
18  
19  
20  
21  
22  
23  
24  
25  
26  
27  
28  
29  
30  
31  
32  
33  
34  
35  
36  
37  
38  
39  
40  
41  
42  
43  
44  
45  
46  
47  
48  
49  
50  
51  
52  
53  
54  
55  
56  
57  
58  
59  
60

## TOC (Table of Contents) Graphic



Vitamin E  
relieves  
compressive  
packing stress